Communication

# Activation of High-*T* Ferromagnetism in Mn-Doped ZnO using Amines

Kevin R. Kittilstved, and Daniel R. Gamelin

*J. Am. Chem. Soc.*, **2005**, 127 (15), 5292-5293• DOI: 10.1021/ja050723o • Publication Date (Web): 22 March 2005

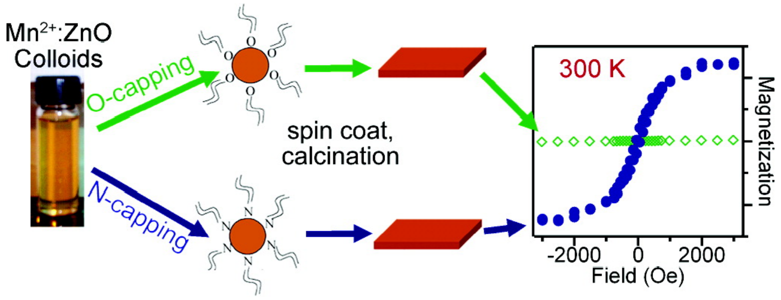

Journal of the American Chemical Society is published by the American Chemical Society. 1155 Sixteenth Street N.W., Washington, DC 20036

J|A|C|S
COMMUNICATIONS

# Activation of High-$T_C$ Ferromagnetism in $Mn^{2+}$-Doped ZnO using Amines

Kevin R. Kittilstved and Daniel R. Gamelin*
*Department of Chemistry, University of Washington, Seattle, Washington 98195-1700*

Received February 3, 2005; E-mail: Gamelin@chem.washington.edu

Since its discovery in $Co^{2+}$-doped $TiO_2$ in 2001,[1] high-Curie temperature ($T_C$) ferromagnetism has been observed in a number of diluted magnetic oxides (DMOs),[2] and elucidation of its origins has been cited as among the most important problems in magnetism to have emerged in several years.[3,4] Identification of the critical parameters governing DMO ferromagnetism has been challenging, however, and often different laboratories have reported incongruous results for seemingly identical materials. For example, high-$T_C$ ferromagnetism in p-type $Mn^{2+}$:ZnO was predicted theoretically,[5−8] but many groups have observed only paramagnetism.[9−11] Since the first claim of room-temperature ferromagnetism in $Mn^{2+}$:ZnO (ferromagnetic saturation moment $M_S(300\ K) \approx 0.16\ \mu_B/Mn^{2+}$),[12] high-$T_C$ ferromagnetism has been observed in $Mn^{2+}$:ZnO/GaAs films that appeared to correlate with p-type conductivity,[13] but near-room-temperature ferromagnetism was also claimed for n-type $Mn^{2+}$:ZnO.[14] Recently, ferromagnetism described earlier as intrinsic was suggested to instead arise from manganese oxide impurity phases, such as Zn-doped $Mn_2O_3$ or $Mn_3O_4$.[15,16] Here, we report that high-$T_C$ ferromagnetism in $Mn^{2+}$:ZnO can be activated reliably by amine binding and calcination, a process interpreted as incorporating nitrogen into the ZnO lattice as a p-type dopant. These results clearly demonstrate that $Mn^{2+}$:ZnO ferromagnetism is critically sensitive to defects other than the magnetic dopants themselves, offering some insight into the otherwise irreconcilable observations reported previously.

We recently reported high-$T_C$ ferromagnetism in $Mn^{2+}$:ZnO prepared by direct chemical synthesis.[17] To explain the large $M_S$ of 1.35 $\mu_B/Mn^{2+}$, we speculated that calcination of amines may introduce p-type nitrogen defects into the ZnO lattice. To test this hypothesis, we have performed the split-batch experiment described by Figure 1.[18] A single batch of high-quality 0.20% $Mn^{2+}$:ZnO nanocrystals[17] was split into two equal parts. Half were capped with trioctylphosphine oxide (TOPO, O-capped), and the other half were capped with trioctylamine (N-capped) under identical conditions. Clear colloidal suspensions of the nanocrystals in toluene were spin coated onto fused-silica substrates and calcined aerobically at 500 °C for 2 min per coat (∼20 coats total, 1 μm thickness). Figure 1 shows 300 K magnetization loops collected for the two films. Whereas the sample prepared from O-capped nanocrystals showed little magnetization at 300 K, that prepared from N-capped colloids showed a strong magnetic hysteresis with $M_S = 1.22\ \mu_B/Mn^{2+}$ and a coercivity of 65 Oe. This experiment was repeated several times with various N (dodecylamine or trioctylamine) or O (TOPO or acetate) ligands. Without exception, N-capped colloids yielded ferromagnetic films (13 films, mean $M_S(300\ K) = 0.76 \pm 0.42\ \mu_B/Mn^{2+}$), whereas O-capped colloids yielded paramagnetic films (10 films, mean $M_S(300\ K) = 0 \pm 0\ \mu_B/Mn^{2+}$). Calcined powders gave similar results.

Figure 2a shows magnetization data measured as a function of temperature for representative ferromagnetic and paramagnetic samples. The data from the paramagnetic sample are reproduced well by a $S = {}^5/_2$ Brillouin function[17] using the analytical $Mn^{2+}$ concentration determined by atomic emission spectrometry and no variable parameters. This agreement demonstrates that manganese oxides are not formed during calcination since, in that case, the $S = {}^5/_2$ paramagnetism would be reduced. Indeed, the concentration of $Mn^{2+}$ (0.20%) is ca. $10^2$ times lower than its solid solubility under these conditions (∼20%).[19] In addition to paramagnetism, the ferromagnetic sample shows a large temperature-independent moment that persists up to the instrument limit of 350 K. This signal is the ferromagnetism shown in Figure 1, and its temperature independence demonstrates $T_C \gg 350$ K.

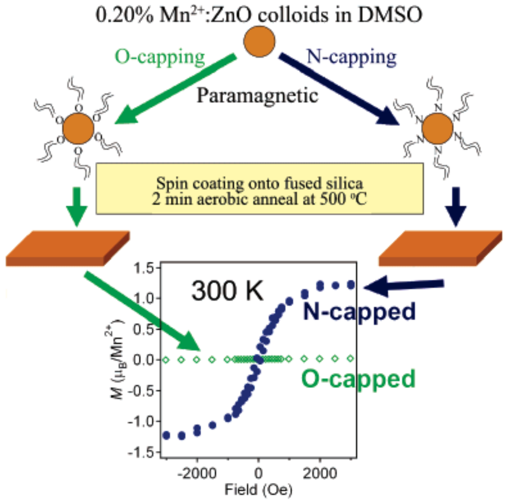

***Figure 1.*** Split-batch experiment; 300 K magnetization data for films spin coated from N-capped (●) and O-capped (◇) $Mn^{2+}$:ZnO colloids taken from the same synthesis batch. See Supporting Information for experimental details.

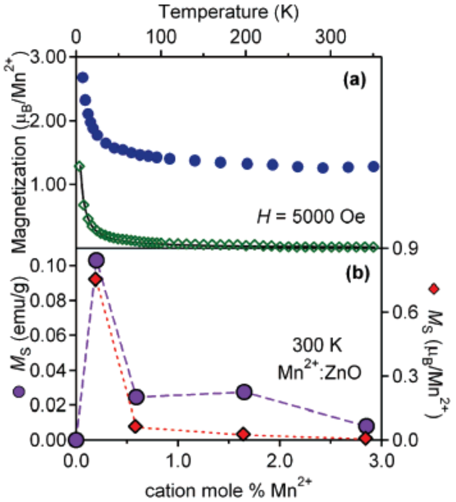

***Figure 2.*** (a) Variable-temperature magnetization data for 0.20% $Mn^{2+}$:ZnO samples prepared from N-capped (●) and O-capped (◇) colloids, collected at 5000 Oe to reveal the paramagnetism. The solid line in (a) was calculated from the $S = {}^5/_2$ Brillouin function, as described in the text. (b) $M_S(300\ K)$ as a function of $Mn^{2+}$ concentration, represented in units of emu/g (●) and mB/$Mn^{2+}$ (▲).

10.1021/ja050723o CCC: $30.25

***Scheme 1***

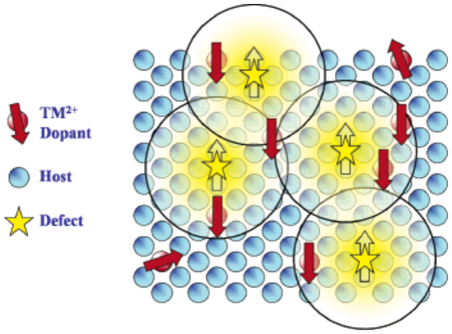

Figure 2b shows the dependence of the 300 K ferromagnetism on $Mn^{2+}$ concentration for a series of samples prepared under identical conditions. These data show that $Mn^{2+}$ is required, but that increasing its concentration above 0.20% actually reduces both $M_S/Mn^{2+}$ and $M_S$/g, inconsistent with scenarios involving ferromagnetism from segregated manganese oxides. A similar concentration dependence in n-type DMOs has been rationalized by invoking formation of antiferromagnetically coupled $TM^{2+}$ dimers.[4] From 0.20 to 1.0%, the statistical probability that a $Mn^{2+}$ ion is isolated without any nearest neighbor $Mn^{2+}$ ions decreases by only 16% (from 98 to 82%),[20] however, a difference far too small to account for the 97% reduction in ferromagnetism over the same concentration range, arguing against this explanation in the present case. This concentration dependence likely reflects the relative availability of nitrogen[8] (vide infra) and is the subject of ongoing investigation.

We attribute the activation of ferromagnetism in $Mn^{2+}$:ZnO to the incorporation of uncompensated p-type defects into the ZnO lattice upon amine calcination, a process that has substantial precedence in the literature surrounding p-type ZnO. Successful methods for preparing p-type ZnO have largely relied on introduction of NO, $NH_3$, $N_2$, or $N_2O$ during[21] or after[22] vacuum deposition to incorporate nitrogen, believed from single-crystal EPR data to substitute for lattice oxygen as the reduced shallow acceptor, $N_O^{3-}$.[21] Three factors likely contribute to the successful incorporation of uncompensated p-type defects in our $Mn^{2+}$:ZnO samples. (1) Amine capping forms $Zn^{2+}-N_{amine}$ bonds, providing activated nitrogen already bound to lattice cations. (2) Aerobic synthesis and calcination aid suppression of native donor defects, such as $O_V$, $Zn_i$, or H.[21] (3) Amine capping passivates surface defects that could otherwise be trapped during sintering (evident from the diminished green defect emission and enhanced UV excitonic emission in N-capped ZnO nanocrystals[17]). We note that addition and calcination of amines after spin coating also enhances the ferromagnetism of the $Mn^{2+}$:ZnO films.

The experimental observations are consistent with a microscopic mechanism involving formation of bound magnetic polarons (BMPs)[23] upon introduction of p-type dopants, analogous to that proposed recently for n-type DMOs.[4] Magnetic exchange interactions between defect-bound VB holes and $Mn^{2+}$ ions occupying the same space are proposed to align $Mn^{2+}$ spins with respect to one another, forming a BMP. As the defect density is increased, overlapping BMPs coalesce into an extended ferromagnetic domain, as illustrated in Scheme 1.[4] The hole$-Mn^{2+}$ exchange energy ($N_0\beta$) arises from oxo(p)$-Mn^{2+}$(d) covalency and can be parametrized using the configuration interaction expression in eq 1,[24] in which the resonance integral is proportional to the spatial overlap (Scheme 1), $S$ is the dopant spin, and $E^-$ represents the energy associated with transfer of the VB hole to $Mn^{2+}$ ($E^+$ for transfer of a VB electron to $Mn^{2+}$).

$$N_0\beta = -\frac{16\langle\psi_{VB}|\hat{H}_{pd}|\psi_{3d}\rangle^2}{S}\left[\frac{1}{E^-}+\frac{1}{E^+}\right] \qquad (1)$$

By MCD spectroscopy, the $Mn^{2+} \rightarrow Mn^{3+}$ photoionization transition in $Mn^{2+}$:ZnO has been identified at 24 000 $cm^{-1}$,[17] just 4000 $cm^{-1}$ below the VB → CB excitation, implying that $E^-$ is very small (~4000 $cm^{-1}$). The strong hole$-Mn^{2+}$ hybridization that results promotes long-range $Mn^{2+}-Mn^{2+}$ exchange coupling (Scheme 1). This analysis is supported by density functional calculations of $Mn^{2+}$:ZnO band structure.[6-8] When p-doped, delocalization of VB holes onto $Mn^{2+}$ ions is extensive and the wave function at the Fermi level possesses substantial manganese character. Hybridization at the Fermi level is the source of all potential spintronics applications of this material.

In summary, we report the discovery that calcination of amines activates high-$T_C$ ferromagnetism in $Mn^{2+}$:ZnO. Perhaps the most important aspect of this result is the clear demonstration that the magnetism of $Mn^{2+}$:ZnO (and by inference, other DMOs) is critically dependent upon factors other than the transition metal dopants themselves. Such factors are likely responsible for the broad range of magnetic properties previously reported.

**Acknowledgment.** This work was funded by the NSF (DMR-0239325 and ECS-0224138). D.R.G. is a Cottrell Scholar of the Research Corporation. Paul Archer (U.W.) is thanked for preliminary magnetic measurements.

**Supporting Information Available:** Experimental details and additional materials characterization (2 figures). This material is available free of charge via the Internet at http://pubs.acs.org.

## References

(1) Matsumoto, Y.; Murakami, M.; Shono, T.; Hasegawa, T.; Fukumura, T.; Kawasaki, M.; Ahmet, P.; Chikyow, T.; Koshihara, S.; Koinuma, H. *Science* **2001**, *291*, 854.
(2) For a recent review of DMOs, see: Pearton, S. J.; Heo, W. H.; Ivill, M.; Norton, D. P.; Steiner, T. *Semicond. Sci. Technol.* **2004**, *19*, R59.
(3) Dietl, T. *Nat. Mater.* **2003**, *2*, 646.
(4) Coey, J. M. D.; Venkatesan, M.; Fitzgerald, C. B. *Nat. Mater.* **2005**, *4*, 173 and references therein.
(5) Dietl, T.; Ohno, H.; Matsukura, F.; Cibert, J.; Ferrand, D. *Science* **2000**, *287*, 1019.
(6) Sato, K.; Katayama-Yoshida, H. *Physica E* **2001**, *10*, 251.
(7) Wang, Q.; Sun, Q.; Jena, P.; Kawazoe, Y. *Phys. Rev. B* **2004**, *70*, 052408.
(8) Petit, L.; Schulthess, T. C.; Svane, A.; Temmerman, W. M.; Szotek, Z. *Mater. Res. Soc. Symp. Proc.* **2004**, *825E*, G2.9.1.
(9) Gratens, X.; Bindilatti, V.; Oliveira, N. F., Jr.; Shapira, Y.; Foner, S.; Golacki, Z.; Haas, T. E. *Phys. Rev. B* **2004**, *69*, 125209.
(10) Han, S.-J.; Jang, T.-H.; Kim, Y. B.; Park, B.-G.; Park, J.-H.; Jeong, Y. H. *Appl. Phys. Lett.* **2003**, *83*, 920.
(11) Yoon, S. W.; Cho, S.-B.; We, S. C.; Yoon, S.; Suh, B. J.; Song, H. K.; Shin, Y. J. *J. Appl. Phys.* **2003**, *93*, 7879.
(12) Sharma, P.; Gupta, A.; Rao, K. V.; Owens, F. J.; Sharma, R.; Ahuja, R.; Osorio Guillen, J. M.; Johansson, B.; Gehring, G. A. *Nat. Mater.* **2003**, *2*, 673.
(13) Lim, S.-W.; Jeong, M.-C.; Ham, M.-H.; Myoung, J.-M. *Jpn. J. Appl. Phys.* **2004**, *43*, L280.
(14) Heo, Y. W.; Ivill, M. P.; Ip, K.; Norton, D. P.; Pearton, S. J.; Kelly, J. G.; Rairigh, R.; Hebard, A. F.; Steiner, T. *Appl. Phys. Lett.* **2004**, *84*, 2292.
(15) Kundaliya, D. C.; Ogale, S. B.; Lofland, S. E.; Dhar, S.; Metting, C. J.; Shinde, S. R.; Ma, Z.; Varughese, B.; Ramanujachary, K. V.; Salamanca-Riba, L.; Venkatesan, T. *Nat. Mater.* **2004**, *3*, 709.
(16) Zheng, R. K.; Liu, H.; Zhang, X. X.; Roy, V. A. L.; Djurisic, A. B. *Appl. Phys. Lett.* **2004**, *85*, 2589.
(17) Norberg, N. S.; Kittilstved, K. R.; Amonette, J. E.; Kukkadapu, R. K.; Schwartz, D. A.; Gamelin, D. R. *J. Am. Chem. Soc.* **2004**, *126*, 9387.
(18) See Supporting Information for experimental details.
(19) White, W. B.; McIlvried, K. E. *Trans. Brit. Ceram. Soc.* **1965**, *64*, 521.
(20) Bryan, J. D.; Gamelin, D. R. *Prog. Inorg. Chem.* **2005**, *54*, 47.
(21) Look, D. C.; Claflin, B. *Phys. Status Solidi B* **2004**, *241*, 624.
(22) Rommeluère, J. F.; Svob, L.; Jomard, F.; Mimila-Arroyo, J.; Lusson, A.; Sallet, V.; Marfaing, Y. *Appl. Phys. Lett.* **2003**, *83*, 287.
(23) Furdyna, J. K.; Kossut, J. Diluted Magnetic Semiconductors. In *Semiconductors and Semimetals*; Academic Press: New York, 1988; Vol. 25.
(24) Bhattacharjee, A. K. *Phys. Rev. B* **1992**, *46*, 5266.

JA050723O